A novel approach for predicting P-glycoprotein (ABCB1) inhibition using molecular interaction fields

Published in final edited form as:
J Med Chem. 2011 March 24; 54(6): 1740–1751. doi:10.1021/jm101421d.

A Novel Approach for Predicting P-glycoprotein (ABCB1) Inhibition Using Molecular Interaction Fields

Fabio Broccatelli[a], **Emanuele Carosati**[a], **Annalisa Neri**[b], **Maria Frosini**[b], **Laura Goracci**[c], **Tudor I. Oprea**[d], and **Gabriele Cruciani**[a,*]

[a]Laboratory of Chemometrics, Department of Chemistry, University of Perugia, Via Elce di Sotto 10, I-06123 Perugia, Italy

[b]Department of Neuroscience, Pharmacology Unit, University of Siena, Siena, Italy

[c]Molecular Discovery Limited, 215 Marsh Road, Pinner, Middlesex, London HA5 5NE, United Kingdom

[d]Division of Biocomputing, Department of Biochemistry and Molecular Biology, University of New Mexico School of Medicine, MSC11 6145, Albuquerque, NM 87131, USA

Abstract

P-glycoprotein (Pgp or ABCB1) is an ABC transporter protein involved in intestinal absorption, drug metabolism and brain penetration, and its inhibition can seriously alter a drug's bioavailability and safety. In addition, inhibitors of Pgp can be used to overcome multidrug resistance. Given this dual-purpose, reliable in silico procedures to predict Pgp inhibition are of great interest. A large and accurate literature collection yielded more than 1200 structures; a model was then constructed using various MIF-based technologies, considering pharmacophoric features and those physico-chemical properties related to membrane partitioning. High accuracy was demonstrated internally, with two different validation sets, and moreover using a number of molecules, for which Pgp inhibition was not experimentally available but was evaluated `in-house'. All the validations confirmed the robustness of the model and its suitability to help medicinal chemists in drug discovery. The information derived from the model was rationalized as a pharmacophore for competitive Pgp inhibition.

Introduction

Minimizing failures in early phases is one of the main strategies in current drug discovery. While in the period between 1964–1985 poor pharmacokinetic properties were the major reason for drug failures, in the last two decades safety, together with lack of efficacy, have become a main concern. In particular, human adverse drug reactions (ADRs) have emerged as the principal reason for drugs withdrawal from the market over the past 20 years.1 Rarely occurring ADRs may explain why potentially toxic effects of drugs were not detected during clinical trials. Rationalization of these failures led to the identification of a number of antitargets, namely those targets which, upon interaction with therapeutic drugs, may result

*CORRESPONDING AUTHOR FOOTNOTE Prof. Gabriele Cruciani, Laboratory for Chemometrics and Cheminformatics, Department of Chemistry, University of Perugia, Italy. Tel: +39 (0)75 5855550; Fax: +39 (0)75 45646 gabri@chemiome.chm.unipg.it.

Supporting Information IUPAC names and SMILES codes for the collected data; options for the calculations of Volsurf+ and Flap; details (Q^2 and R^2) of the PLS models; details of statistics (True Positives, True Negatives, False Positives, False Negatives) for the Training set, the Internal Validation set, and the External Validation set; analysis of chemical space of compounds from the Training set and the Validation sets; experimental data demonstrating the purity of the active compounds. This material is available free of charge via the Internet at http://pubs.acs.org.

in severe ADRs.2 ABCB1, also known as P-glycoprotein, Pgp or MDR1, is a membrane protein member of the ATP-binding cassette (ABC) transporters superfamily. Together with hERG channel and CYP3A4, it is probably the most widely studied antitarget.

P-glycoprotein is expressed in a variety of human tissues as defense against xenobiotics. It uses energy derived by ATP hydrolysis to translocate its ligands out of the cell against the concentration gradient. Pgp is probably the most promiscuous efflux transporter, since it recognizes a number of structurally different and apparently unrelated xenobiotics; notably, many of them are also CYP3A4 substrates. CYP3A4 and ABCB1 are often expressed in the same tissues, hence for common substrates the amount of efflux determines the exposure to metabolism.[3] This interplay affects bioavailability of drugs co-administered with a Pgp inhibitor or inducer.[4,5]

Pgp is also an interesting target in oncology,[6] since multidrug resistance is often associated with its overexpression. Therefore, potent selective Pgp inhibitors have been rationalized as adjuvant therapy when co-administered with anti-cancer drugs. Until now, a number of candidates failed clinical trials due to poor selectivity. In particular, first generation chemosensitizers, generally drugs known to be active toward other targets, were ineffective at non-toxic concentrations, while second generation chemosensitizers often failed because of simultaneous Pgp and CYP3A4 inhibition.[7]

Pgp awareness should be routinely included in the early phases of drug discovery,[8] given its duality as target and antitarget.9 Reliable in vitro assays to evaluate the Pgp inhibition capability of new drug entities are costly and time demanding, so the integration of in silico and in vitro procedures can help to minimize the costs. For this reason a number of in silico models for recognition of Pgp substrates and inhibitors have been proposed in recent years. Lack of a high-resolution crystal structure for human Pgp, together with the high flexibility of ABC transporters, justify the prevalence of ligand-based models.10 Statistics and information gained from these models were recently reviewed in extenso.11,[12] The reviewed Pgp inhibition models generally agreed on the utility of pharmacophoric descriptors, and consistently identified the importance of a hydrogen bond (HB) acceptor coupled with some hydrophobic regions (between two and four). Although these models shared good interpretability, they demonstrated diminished performance when tested against non-local external validation sets. On the other hand, classification models using non-pharmacophoric description often showed better predictive power for Pgp substrate recognition, but were rarely used to discriminate inhibitors from non-inhibitors.

It is preferable for in silico models to rely upon on an extensive data collection that allows an appropriate chemical space coverage, combined with appropriate molecular descriptors. In this work a thorough literature analysis yielded a training set of 772 molecules and two validation sets, composed of molecules taken either from the same references of the training set (with inherent chemical space bias), or from articles not used for the training set collection (i.e. different chemotypes). In addition, different classes of molecular description were evaluated, in order to account for non-specific factors such as water solubility and membrane partitioning and for more specific pharmacophoric features responsible for ligand-protein interactions.

In particular, molecules described using GRID Molecular Interaction Field (MIF)[13–15] approaches resulted in a “Composite model” for Pgp inhibition, based on an intuitive pipeline of preceding “local models” developed for competitive or non-competitive binding. VolSurf+ descriptors16–18 were used to model physicochemical properties, whereas the pharmacophoric method FLAP[19–21] was employed to superimpose molecules and evaluate their MIF similarity. With VolSurf+, a number of important parameters were detected for

Pgp inhibition, while FLAP identified the most important pharmacophoric features around the optimal molecular shape. The emergent model can be used to predict Pgp inhibition and to guide compound design to modulate its impact within series of molecules.

Results

Data Collection

The collected data (available as Supporting Information) refers to the inhibition of transport of an ABCB1 probe substrate in a cell line expressing Pgp. For compound categories we observed the definitions of Rautio *et al.*, who tested some molecules with different protocols and derived qualitative rules to classify Pgp inhibitors.[22] Thus, inhibitors having IC_{50} lower than 15 μM may be involved in drug-drug interactions, whereas those with an IC_{50} higher than 100 μM are considered not inhibitors. Molecules having an IC_{50} of between 15 and 100 μM are classified as weak inhibitors. Different protocols revealed that some inhibitors (IC_{50} lower than 15 μM) and non-inhibitors fall in the "grey region" of weak inhibitors when experimental conditions were altered.[22] These compounds were excluded from our set. On the contrary, a "two-class jump" (from inhibitor to non- inhibitor) was rarely observed, e.g. for 9-hydroxy-Risperidone.[23,24]

To enlarge our dataset we extended the qualitative classification to all those molecules for which activity was reported as percentage of inhibition. Thresholds values for percentage of inhibition were defined through pairwise comparison based on those structures for which both IC_{50} and percentage were available (see Table 1).

Molecules with molecular weight >700 were not used to avoid inappropriate coverage of the chemical space. Rules for categorization were applied to data from 44 publications, resulting in a set of 857 molecules, which were then divided into a "Training Set" (N=772) and an "Internal Validation Set" (N=85), as illustrated in Figure 1.[22–65] The Internal Validation Set was extracted from a Principal Component Analysis (PCA) computed in Volsurf+ using the Most Descriptive Compounds (MDC) algorithm for subset selection. This set was used to evaluate predictive performance of the model against known near-neighbor molecules (biased predictions).

A second "External Validation Set" was extracted from Wombat,[66] Chembl[67] and Klopman[68] data sets, excluding the molecules already present in our collection. Since Klopman *et al.* tested molecules for Multidrug Resistance and not specifically for Pgp inhibition, only those [not reversing] multidrug resistance (R-FOLD=1) were used. At the end, the External Validation Set was composed of N=418 molecules from 17 different references.[68–84] Projecting these molecules in the chemical space of the Training set (using Volsurf+ descriptors and Principal Component Analysis) confirmed that the chemical space of the two sets was only partially overlapping (projections are given as Supporting Information). This set was used to evaluate predictive performance of the model against unknown chemotypes (non-local, or unbiased predictions).

The Model

Molecules were imported into VolSurf+ as SMILES (mostly taken from PubChem85 and Wombat66); some were manually input via the Volsurf+ chemical sketcher.16 Molecular descriptors obtained with VolSurf+ and the pharmacophoric description obtained with FLAP19 were generated for the neutral species, since Ecker confirmed the role of potentially positive (basic) nitrogen as HB acceptor.[86]

Both methods use GRID molecular interaction fields (MIF),[14,15] extracting and processing the information contained therein in different and complementary ways. GRID MIFs have

been applied to many areas of drug discovery,[15,87,88] including pK_a and tautomer modeling,[89,90] structure-based drug design,[91] scaffold-hopping,[92–94] 3D-QSAR,[95–98] docking,[98,99] ADME and pharmacokinetic modeling,[17,18,100] and metabolism prediction.[101–102]

Multivariate methods such as PCA or PLS are the proper way to elaborate pattern recognition or to study quantitative structure-activity relationships, respectively, when the molecules are described by means of Volsurf+ descriptors. A single conformation is typically used for modeling each molecule; however, due to the nature of descriptors, VolSurf+ is mostly conformation-independent. VolSurf+ molecular descriptors refer to molecular size and shape, to size and shape of hydrophilic and hydrophobic regions, and to the balance between them. MIFs from the OH2 and DRY GRID probes are used to define the hydrophilic and hydrophobic regions, respectively; however, the specification in the molecule of HB donor/acceptor character of polar regions, available using the GRID probes O and N1, can be significant in certain cases. VolSurf+ descriptors have been presented in detail elsewhere.[17,18]

In the FLAP approach, originally conceived for[19–21] and successfully applied to virtual screening,[103–107] molecules are stored in a database together with their MIFs, which are condensed into discrete points and exhaustively combined to produce quadruplets, or 4-point pharmacophores. Molecules are compared pairwise, with the quadruplets of each database molecule (ligand) being compared with the quadruplets of the reference structure (molecular template). When a search is performed, all of the quadruplets from the ligand are searched against all of the quadruplets in the template; quadruplets that match are then used to overlay the ligand onto the template. For each alignment, MIF similarity scores are used as a measure of the superimposition between the ligand MIF and the template MIF. A score can refer to the best alignment of two molecules according to a single probe, but two or more probes can be handled as well; in this case, the product of the probe scores is used to select the orientation that simultaneously represents the best MIF alignment of the given probes. The best similarity value for each MIF type produced by a single conformer is retained for each molecule.

Many flavones and steroids, which are non-competitive Pgp inhibitors,[108] were found as outliers by both VolSurf+ and FLAP preliminary models. Thus, 94 molecules with at least one of these chemotypes (flavone-like and steroid-like) were identified among the Training Set and were used to compute a “local model” with the same methodologies used for the Training Set. Attempts to define a pharmacophore model for such a set of compounds (using the same procedure described below for the larger training set) were not as satisfactory as expected; the presence of two different suspect substructures is likely to affect the pharmacophore modeling (with FLAP, whereas it was possible to obtain a model with VolSurf+). In particular, the VolSurf+ model was based on the first two latent variables (LVs), indicating a determinant role for the descriptors of hydrophobicity and permeability (D3, LogPn-oct), which are directly related to Pgp inhibition, and an inverse correlation with aqueous solubility (SOLY).

The remaining 772 Training Set molecules (not containing flavones and steroid chemotypes) were used to derive a Volsurf+ based Partial Least Square Discriminant (PLS-D) model. The model was based on five LVs (Q^2 and R^2 are given as Supporting Information). In particular, HSA, LogPn-oct and descriptors of size (such as molecular surface), were relevant for the first LV, whereas the second and the third reported the importance of flexibility (FLEX), hydrophilic volume (W1), the pharmacophoric descriptor DRDRAC, which is the area between two hydrophobic atoms and one HB acceptor atom (second LV) and the “integy moment” IW4, which refers to the localisation of hydrophilic regions (third

LV). Finally, the fourth and the fifth LVs suggested a determinant role of the charged state (L1lgS in the fourth LV, NCC in the fifth LV, %FU4–10 in both) and hydrophilic capacity factors (in the fourth LV).

The same Training Set molecules were used as input for a Linear Discriminant Analysis (LDA) model for Pgp inhibition with FLAP. The automated procedure available in FLAP selected the chemosensitizer Biricodar among twenty potent Pgp inhibitors candidate templates, and a combination of the GRID probes H, DRY, O and N1 was selected to compute the optimal LDA model. Once a predictive model was computed based on the fields derived by all the atoms of the template, the FLAP module for the selective pharmacophore extraction was applied. In this procedure, the software selects a number of defined features that are important for the LDA model. This model uses only the fields of the selected atoms, together with the shape of the template. Thus, a pharmacophore composed of one HB acceptor, two large hydrophobic regions and molecular shape was created for the competitive binding. The model was based on the FLAP scores H, H*N1, and DRY. Surprisingly, the probe shape (H) was the most relevant, contributing similiarity information to the model alone, and in combination with the N1 probe.

All these models were linked into a “composite model”. The pipeline is briefly reported below and schematized in Figure 3. As a first step, when the substructure search reveals the presence of suspect chemotypes, non-competitive binding is evaluated and molecules are classified either as inhibitors or passed further to the competitive binding module. Thus, the combined VolSurf+ and FLAP models evaluate molecules that are less likely to act as non-competitive inhibitors, which are then classified as Pgp inhibitors or non-inhibitors.

The use of accuracy, sensitivity and specificity is commonly accepted to evaluate the capabilities and performance of classification models. In our classification system, sensitivity measures how a model is able to classify inhibitors, specificity measures how a model is able to classify non-inhibitors, whereas accuracy measures how a model is able to classify all the compounds, both inhibitors and non-inhibitors. Table 2 reports the performances of the model in the Training set, the Internal Validation set and the External Validation set.

A final “blind” validation set was composed of a set of eight compounds picked among a data set of about 2,700 drugs, from an in-house historical collection (DRUGS database). All of the compounds already present in our Pgp collection were excluded, with the only exception of Alprenolol (well known Pgp non-inhibitor) and Cyclosporine A (well known Pgp inhibitor) which were included as a negative and positive control, respectively. The remaining molecules of the large data set were projected onto the models and classified either as Pgp inhibitors or non-inhibitors. A snapshot of the prediction is reported in Figure 4: interestingly, 21.5% of the molecules were predicted as potential Pgp inhibitors, which reflects the known high promiscuity of Pgp. Both methods contributed to the prediction of Pgp inhibitors, however Volsurf+ was more selective in classifying compounds as non-inhibitors.

To make a blind selection, a random choice of two and six molecules was performed among those predicted as non-inhibitors or inhibitors, respectively. These eight molecules, together with Cyclosporine A (positive control) and Alprenolol (negative control) were analyzed experimentally to evaluate whether they inhibit human Pgp. The ability of these compounds to inhibit Pgp-mediated cell efflux of R123 in mouse T lymphoma L5178 MDR1 cells was studied. Alprenolol (control), Ticarcillin and Nateglinide were not effective, while all the other molecules tested are effective. In particular, Aprindine and Ziprasidone are weak inhibitors, Sertindole was characterized by α_{max} of 0.74 at the concentration of 1×10^{-4} M

(apparent IC_{50} value of 6.5×10^{-6} M) whereas Ebastine and Aripiprazole turned out to be efficacious Pgp inhibitors, with α_{max} values close to 1 and IC_{50} value of 1.5×10^{-6} and 7.8×10^{-7} M, respectively. Both these compounds were found to be almost equipotent to Cyclosporine A.

Comparison with Other Methods

The Tanimoto similarities to the Pgp inhibitors Biricodar, Zosuquidar, Verapamil and Elacridar were calculated for each molecule in the Dataset using the software Open Babel.[109] The resulting scores were processed using the *k* Nearest Neighbor algorithm implemented in the open source data-mining software Orange Canvas.[110] The euclidean distance was used as a distance metric and the *k* number of neighbors selected was 7. Parameters were selected on the basis of their performance on the training set and in internal validation. Predictions in leave-one-out on the Training set reached a classification accuracy of 0.76. The accuracy of the Internal Validation set was 0.78, while for the External Validation set the accuracy of the 2D method dropped to 0.59. Finally, out of the blind set the only Ebastine (Pgp inhibitor) and Ziprasidone (weak inhibitor) were predicted as Pgp inhibitors, whereas all the remaining molecules were predicted to be Pgp non-inhibitors.

Discussion

A novel approach for predicting P-glycoprotein (ABCB1) inhibition using GRID molecular interaction fields is reported. Instead of using one of the current literature collections available, an exhaustive literature search was performed, based on an accurate data analysis and on a straightforward way to categorize molecules as inhibitors and or non-inhibitors. More than 1,200 molecules were collected and structured into three data sets: the Training set and the Internal Validation set were extracted from the same 44 references (therefore sharing the same chemical space), whereas the External Validation set was derived from an additional 17 references.

The second step of the work focused on molecular description. Most in silico procedures for Pgp inhibitors recognition proposed in the past exclusively employed pharmacophoric descriptors, without considering descriptors typically related to ADME properties (e.g. membrane permeability). These models generally agree on the importance of HB acceptors and aromatic or hydrophobic features as a driving force for Pgp inhibition. The role of nitrogen as a HB acceptor has been experimentally confirmed, suggesting that molecules should be modeled in their neutral form.[86] Unfortunately, even when exhibiting good interpretability, pharmacophore models rarely reached high accuracy when applied to large datasets with non-local series. This suggests that a pharmacophore for Pgp inhibition is a necessary but not sufficient condition. Hence VolSurf+ molecular descriptors, optimized to model pharmacokinetic properties, were used in tandem with a pharmacophoric method (FLAP).

In a recent review Leach asserts that pharmacophoric hypotheses arise from the process of elucidation, defined as “the identification from a set of active molecules and their biological activities of the key common features and their relative orientations”; as Leach emphasizes, the process is dependent on the alignment of active molecules, that is the key step.[111] In this sense FLAP can be considered as pharmacophore-based, since all Training Set molecules are superimposed to a template's conformation and then GRID MIF similarity is calculated. Among the resulting scores, only a reduced number are subsequently employed in a Linear Discriminant Analysis. These are considered by FLAP the crucial features for the biological activity.

Using FLAP to define the pharmacophore it is possible to localize, orientate and confine the features supposed to be biologically essential. Interestingly, all the inhibitors in our data set have at least one HB acceptor atom, while there are some without HB donors. Particularly significant is the example of the tertiary amine Amitriptyline, an inhibitor with only one heteroatom,[42] which leads to the minimalistic hypothesis of a pharmacophore with a unique HB acceptor atom, one or two hydrophobic and/or aromatic features and no HB donor atoms.

Based on the FLAP alignment, we hypothesize that an optimal shape for Pgp inhibitors may exist. Molecules in a conformation that sufficiently fits the optimal shape can be classified as Pgp inhibitors when they also have hydrophobic and HB acceptor characteristics (i.e., MIFs) that have a good similarity to that of the template's. The pharmacophore, reported in Figure 6, can be summarized as an ensemble of cavity-shape plus one hydrogen bond acceptor atom and one large hydrophobic region, together consistent with the minimalistic hypothesis reported above. It is interesting to note than almost 90% of all the inhibitors, small medium and large, fit this simple pharmacophoric hypotesis.

Notably, the use of molecular shape in the FLAP-derived pharmacophore not only fits, but fulfills the IUPAC definition: “A pharmacophore is the ensemble of steric and electronic features that is necessary to ensure the optimal supramolecular interactions with a specific biological target structure and to trigger (or to block) its biological response”.[112]

The precedent use of VolSurf+ descriptors, in agreement with the hypothesis of an important synergistic effect of pharmacokinetic and pharmacodynamic properties, produced a robust model. Descriptors of size, hydrophobic surface area, flexibility and LogPn-oct emerged as strongly significant (see Figure 7). In particular, while molecular surface, flexibility and hydrophobic surface might approximately encode characteristics captured by the FLAP model, LogPn-oct is a well-established membrane permeability descriptor. In fact a certain degree of correlation emerges in the work of Polli *et al.*, where median and minimum permeability are sensibly higher for inhibitors respect to non-inhibitors.[38]

More than 90% of the molecules with a computed LogPn-oct lower than 2 are non-inhibitors (Figure 7). Descriptors of the charged state (e.g. percentage of neutral species at different pH) affected predictions in an opposite manner at the 3th and at the 4th latent variables. This behavior confirms the major role played by basic nitrogens that can easily switch from HB acceptors to HB donors depending on the protonation state. In the preliminary work a conspicuous number of outliers having the flavonoid and steroid chemotypes, respectively, have been detected. These structures had been previously characterized as binders to a cytosolic mouse ABCB1 domain vicinal to the ATP binding-site.[108] Moreover, flavonoids also bind to the cytosolic domain of other proteins (e.g. kinases), and it is therefore not surprisingly that they act in a promiscuous manner.[113] Polli *et al.* previously showed that testosterone non-competitively inhibits Pgp without stimulating ATP hydrolysis.[38] For these reasons a separate local model was built, limited to those molecules containing at least one of an ensemble of substructures characteristic for the flavonoid and steroid chemical classes, respectively. We refer to this model as the non-competitive binding model, for lack of a better description. Permeability and hydrophobicity appear to be determinant, while the contribution of size and flexibility appeared negligible; these results partially agree with the work of Boccard *et al.*[114]

The composite model has high accuracy with a good balance between specificity and sensitivity, suggesting that for comparable physicochemical features the pharmacophore description becomes critical, and vice-versa. Overall, the Volsurf+ and FLAP-based models

are complementary, and were used in combination to provide a highly predictive composite model.

Conclusion

Drug-drug interactions via Pgp inhibition are of great interest in the pharmaceutical sector, as well as drug discovery. Especially when co-administered with a CYP3A4 substrate, a Pgp inhibitor might alter the bioavailability of such substrates, leading to altered pharmacokinetic and pharmacodynamic profiles, as well as overdosing and toxicity. When integrated with in vitro assays, such in silico tools can be valuable during the early drug discovery phases for the early identification of potential drug-drug interactions and toxicity. We developed a novel approach for predicting Pgp inhibition based on the synergistic combination of specific (pharmacophore) and non-specific (general physico-chemical) descriptors. Given the frequent occurrence of Pgp inhibition in new chemical entities, guidelines to reduce toxicity are of great interest. The model presented here suggests that modulation of permeability, flexibility or hydrophobic surface area, might provide ways to overcome this particular issue. For candidates having optimal ADME properties but inhibiting Pgp, minimal structural changes would be required. For this purpose a pharmacophore model for competitive inhibition was elucidated. Interestingly shape appears to emerge as a crucial factor, indicating the importance of the three-dimensional description for antitarget modeling.

From the point of view of Pgp as a target, rather than antitarget, a potent non-toxic inhibitor able to increase the anti-cancer activity of co-administered drugs has yet to be found. Recurrent failures in clinical trials were often related to side effects, since chemosensitizers were initially derived from scaffolds that are active toward other targets.

Since Pgp has dual role as both target and antitarget, the model presented here has double utility, since it can be used to help prevent unwanted effects when evaluating ADME-Tox properties, as well as when searching for new inhibitors when addressing Pgp as target. The performance observed from the training set and validation sets (Internal and External) is supported by a blind prediction, which was confirmed on a set of experimentally tested molecules, since all predictions were correct. Interestingly, the three molecules predicted as non-inhibitors and four of the six predicted as inhibitors were experimentally confirmed, whereas the remaining two are in the range for which we defined the experimental uncertainty for Pgp inhibitor/non-inhibitor classification. We note that two of these newly reported Pgp inhibitors, Ebastine and Aripiprazole, are in the micromolar range.

In conlusion, the uniqueness of the model presented here is the way in which the problem is handled. In fact, the well-known complexity of Pgp inhibition has been split in several issues, which include: cell permeability, pharmacophore identification (for direct binding) and non-competitive binding (probably in the ATP binding site). In this paper we have presented how all these features/issues should be modelled using a sequence of filters and local models and not with a unique model.

Experimental Section

1. Molecules

The molecules of the blind set were purchased from Sigma-Aldrich,[115] with the exception of Cyclosporine, which was purchased from Alexis Biochemicals (San Diego, CA, USA) and Aripiprazole, which was obtained from Sanofi Aventis, Bridgewater, NJ, USA.

Active compounds (Aripiprazole, Ebastine, Sertindole, Repaglinide, Ziprasidone, and Aprindine) have been characterised by mass spectrometry; purity was found to be over 95% for all compounds tested.; the corresponding analytical data have been reported in table S4 of Supporting Information.

2. Cells line and cultures

The L5178Y mouse T-lymphoma cell line transfected with a recombinant MDR1/A retroviral vector (pHa MDR1/A), a generous gift from Dr. Michael M. Gottesman (National Cancer Institute, Bethesda, MD, USA), were used. Human MDR1-expressing cells were selected by culturing the transfected cells with 60 ng/ml colchicine to maintain the expression of the MDR phenotype.[116] The L5178 MDR1 cell line was grown in McCoy's 5A medium supplemented with 10% heat-inactivated horse serum, 2 mM L-glutamine, 100 UI/ml penicillin and 0.01 mg/ml streptomycin. Cells were maintained in a humidified incubator with an atmosphere of 95% air and 5% CO_2 at 37 °C. When the cells reached confluency, they were harvested and plated for subsequent passages (up to 20) and for drug treatment. Cultures were initiated at a density of 2×10^5 cells/ml and grown exponentially to about 2×10^6 cells/ml in 48h. Cells will werebe counted in a Burker cytometer before use and their viability tested by Trypan Blue exclusion.

3. Cell loading with Rhodamine 123 and inhibition of Pgp-mediated Rhodamine 123 efflux assay

The capability of the compounds to inhibit Rhodamine 123 (R123) efflux was determined as already described by Saponara *et al.*[117] with some modifications. Briefly, L5178 MDR1 cells (2×10^6 ml^{-1}) were resuspended in serum-free McCoy's 5A medium, and 0.5 ml aliquots of the cell suspension were distributed into Eppendorf centrifuge tubes. Compounds tested were added at different concentrations and samples were incubated for 10 min at room temperature. Then, R123 was added to the samples at a final concentration of 5×10^{-6} M R123 and cells were incubated for 20 min at 37 °C. Thereafter, cells were washed twice by centrifugation for 5 min at 2,000 g and resuspended in 0.5 ml phosphate-buffered saline (PBS). R123 retained by cells was quantified as fluorescence, using a Becton-Dickinson FACS Calibur flow cytometer (San Josè, CA, USA) equipped with an ultraviolet argon laser (excitation at 488 nm, emission at 530/30 and 585/42 nm band-pass filters). FACS analysis were gated to include only individual, viable cells on the basis of forward and side light-scatter and were based on acquisition of data from 10,000 cells. Fluorescence signals were analyzed by the BDIS CellQuest software (Becton Dickinson, San Josè, CA, USA). The mean fluorescence intensity (MFI) were used for comparison among different conditions. Sodium orthovanadate (Vi) were was selected as the positive control for a standard inhibitor since already at 5×10^{-3} M concentration it can maximally inactivate the Pgp efflux pump.[118] IC_{50} for Vi determined on L5178 MDR1 cells was about 7×10^{-4} M.

4. Data analysis and statistics

Data were reported as mean ± SEM of at least three independent experiments run in triplicate. The fluorescence data were expressed as the mean of arbitrary fluorescence units derived from histogram plots of the 10,000 cells that are examined. The percent Pgp inhibition exerted by a single compound was calculated as described by Wang *et al.*[118] The relative fluorescence (i.e. percent inhibition of Pgp) was calculated as mean fluorescence intensity (MFI) of a discrete sample divided by the MFI in the presence of 5×10^{-3} M Vi, times 100:

Relative fluorescence = [MFI of sample/ (MFI of sample + Vi)] × 100

The denominator represents MFI of the sample when inactivation or complete preclusion of the function of Pgp active efflux is attained. The numerator is the resulting signal caused by test compound inhibiting the function of Pgp active efflux. Pgp blocking activity was described by α_{max}, which expresses the efficacy of the inhibitor and by IC_{50}, which measures its potency. α_{max} varies between 0 (in the absence of the inhibitor) and 1 (when the amount of R123 found in L5178 MDR1 cells is comparable to that determined in the presence of 5×10^{-3} M Vi). IC_{50} measures the potency of the inhibitor and represents the concentration that causes a half-maximal increase (α=0.5) in intracellular concentration of R123. IC_{50} values were obtained by best fitting the concentration-dependent inhibition curves (GraphPadPrism5 program, GraphPad Inc., USA).

Supplementary Material

Refer to Web version on PubMed Central for supplementary material.

Acknowledgments

This work was in part supported by the European Union. FP6 PRIORITY LSH-2005-2.2.0-8: Small-ligand libraries: improved tools for exploration and prospective antitumour therapy. DePPICT Project (Designing Therapeutic Protein-Protein Inhibitors for Brain Cancer Treatments) Contract number: LSHC-CT-2007- 037834 (http://www.deppict.eu/home.jsp). This study was supported, in part, by NIH grant 5U54MH084690-03 (TIO).

Abbreviations

ADRs	adverse drug reactions
Pgp	P-glycoprotein, also known as ABCB1
ABC	ATP-binding cassette
MDR	multiple drug resistance
hERG	human ether-a-go-go-related gene
CYP3A4	cytochrome P450 3A4
HB	hydrogen bond
MIF	molecular interaction field
FLAP	fingerprints for ligands and proteins
MDC	most descriptive compounds
PCA	principal component analysis
HB	hydrogen bond
QSAR	quantitative structure-activity relationship
ADME	absorption, distribution, metabolism, excretion
PLS-D	partial least square discriminant
LV	latent variable
LDA	linear discriminant analysis

References

1. Schuster, D.; Laggner, C.; Langer, T. Antitargets Prediction and Prevention of Drug Side Effects. Vaz, RJ.; Klabunde, T., editors. WILEY-VCH; 2008. p. 3-22.

2. Mannhold, R.; Kubinyi, H.; Folkers, G. Antitargets Prediction and Prevention of Drug Side Effects. Vaz, RJ.; Klabunde, T., editors. WILEY-VCH; 2008. p. XXI-XX.
3. Benet LZ. The drug transporter-metabolism alliance: uncovering and defining the interplay. Mol. Pharmaceutics. 2009; 6:1631–1643.
4. Grover A, Benet LZ. Effects of drug transporters on volume of distribution. AAPS J. 2009; 11:250–261. [PubMed: 19399628]
5. Shutgarts S, Benet LZ. The role of transporters in the pharmacokinetics of orally administered drugs. Pharm. Res. 2009; 26:2039–2054. [PubMed: 19568696]
6. Juliano RL, Ling V. A surface glycoprotein modulating drug permeability in Chinese hamster ovary cell mutants. Biochim. Biophys. Acta. 1976; 455:152–156. [PubMed: 990323]
7. Choi S. ABC transporters as multidrug resistance mechanisms and the development of chemosensitizers for their reversal. Cancer Cell Int. 2005; 5:30. Online. [PubMed: 16202168]
8. Food and Drug Administration, Advisory Committee for Pharmaceutical Science. [accessed April 2010]. http://www.fda.gov/ohrms/dockets/ac/04/slides/2004-4079s1.htm
9. Broccatelli F, Carosati E, Cruciani G, Oprea TI. Transporter-Mediated Efflux Influences CNS Side Effects: ABCB1, from Antitarget to Target. Mol. Inf. 2010; 29:16–26.
10. Klepsch F, Ecker GF. Impact of the Recent Mouse P-Glycoprotein Structure for Structure-Based Ligand Design. Mol. Inf. 2010; 29:276–286.
11. Demel MA, Schwaha R, Krämer O, Ettmayer P, Haaksma EEJ, Ecker GF. In silico prediction of substrate properties for ABC-multidrug transporters. Expert. Opin. Drug. Metab. Toxicol. 2008; 4:1167–1180. [PubMed: 18721111]
12. Crivori, P. Antitargets Prediction and Prevention of Drug Side Effects. Vaz, RJ.; Klabunde, T., editors. WILEY-VCH; 2008. p. 367-397.
13. The GRID package, version 22, is distributed from Molecular Discovery Ltd. http://www.moldiscovery.com
14. Goodford PJ. A Computational Procedure for Determining Energetically Favorable Binding Sites on Biologically Important Macromolecules. J. Med. Chem. 1985; 28:849–857. [PubMed: 3892003]
15. Cruciani, G.; Mannhold, R., editors. Molecular Interaction Fields: Applications in Drug Discovery and ADME Prediction. WILEY-VCH; Weinheim: 2005.
16. The VolSurf+ program, version 1.0.4 is distributed by Molecular Discovery Ltd. http://www.moldiscovery.com
17. Cruciani G, Crivori P, Carrupt P-A, Testa B. Molecular Fields in Quantitative Structure-Permeation Relationships: the VolSurf Approach. THEOCHEM-J. Mol. Struc. 2000; 503:17–30.
18. Crivori P, Cruciani G, Carrupt P-A, Testa B. Predicting blood-brain barrier permeation from three-dimensional molecular structure. J. Med. Chem. 2000; 43:2204–2216. [PubMed: 10841799]
19. FLAP is distributed by Molecular Discovery Ltd. http://www.moldiscovery.com
20. Perruccio, F.; Mason, J.; Sciabola, S.; Baroni, M. FLAP: 4 point pharmacophore fingerprints from GRID. In: Cruciani, G., editor. Molecular Interaction Fields: Applications in Drug Discovery and ADME Prediction. Vol. vol. 27. Wiley-VCH; Weinheim: 2005. p. 83-102.Methods and Principles in Medicinal Chemistry
21. Baroni M, Cruciani G, Sciabola S, Perruccio F, Mason JS. A Common Reference Framework for Analyzing/Comparing Proteins and Ligands. Fingerprints for Ligands And Proteins (FLAP): Theory and Application. J. Chem. Inf. Model. 2007; 47:279–294. [PubMed: 17381166]
22. Rautio J, Humphreys JE, Webster LO, Balakrishnan A, Keogh JP, Kunta JR, Serabjit-Singh CJ, Polli JW. In vitro p-glycoprotein inhibition assays for assessment of clinical drug interaction potential of new drug candidates: a recommendation for probe substrates. Drug Metab. Dispos. 2006; 34:786–792. [PubMed: 16455806]
23. Feng B, Mills JB, Davidson RE, Mireles RJ, Janiszewski JS, Troutman MD, de Morais SM. In vitro P-glycoprotein assays to predict the in vivo interactions of P-glycoprotein with drugs in the central nervous system. Drug Metab. Dispos. 2008; 36:268–275. [PubMed: 17962372]

24. Wang JS, Zhu HJ, Markowitz JS, Donovan JL, DeVane CL. Evaluation of antipsychotic drugs as inhibitors of multidrug resistance transporter P-glycoprotein. Psychopharmacology. 2006; 187:415–423. [PubMed: 16810505]
25. Merlin JL, Guerci A, Marchal S, Missoum N, Ramacci C, Humbert JC, Tsuruo T, Guerci O. Comparative evaluation of S9788, verapamil, and cyclosporine A in K562 human leukemia cell lines and in P-glycoprotein-expressing samples from patients with hematologic malignancies. Blood. 1994; 84:262–269. [PubMed: 7912556]
26. Toffoli G, Simone F, Corona G, Raschack M, Cappelletto B, Gigante M, Boiocchi M. Structure-activity relationship of verapamil analogs and reversal of multidrug resistance. Biochem. Pharmacol. 1995; 50:1245–1255. [PubMed: 7488241]
27. Hofmann J, Gekeler V, Ise W, Noller A, Mitterdorfer J, Hofer S, Utz I, Gotwald M, Boer R, Glossmann H, Grunicke HH. Mechanism of action of dexniguldipine-HCl (B8509-035), a new potent modulator of multidrug resistance. Biochem. Pharmacol. 1995; 49:603–609. [PubMed: 7887974]
28. Dantzig AH, Shepard RL, Cao J, Law KL, Ehlhardt WJ, Baughman TM, Bumol TF, Starling JJ. Reversal of P-glycoprotein-mediated multidrug resistance by a potent cyclopropyldibenzosuberane modulator, LY335979. Cancer Res. 1996; 56:4171–4179. [PubMed: 8797588]
29. Bain LJ, LeBlanc GA. Interaction of structurally diverse pesticides with the human MDR1 gene product P-glycoprotein. Toxicol. Appl. Pharmacol. 1996; 141:288–298. [PubMed: 8917702]
30. Naito M, Tsuruo T. New multidrug-resistance-reversing drugs, MS-209 and SDZ PSC 833. Cancer Chemother. Pharmacol. 1997; 40:20–24.
31. Chiba P, Holzer W, Landau M, Bechmann G, Lorenz K, Plagens B, Hitzler M, Richter E, Ecker G. Substituted 4-acylpyrazoles and 4-acylpyrazolones: synthesis and multidrug resistance-modulating activity. J. Med. Chem. 1998; 41:4001–4011. [PubMed: 9767638]
32. Wandel C, Kim RB, Kajiji S, Guengerich P, Wilkinson GR, Wood AJ. P-glycoprotein and cytochrome P-450 3A inhibition: dissociation of inhibitory potencies. Cancer Res. 1999; 59:3944–3948. [PubMed: 10463589]
33. Golstein PE, Boom A, van Geffel J, Jacobs P, Masereel B, Beauwens R. P-glycoprotein inhibition by glibenclamide and related compounds. Pfluegers Arch. 1999; 437:652–660. [PubMed: 10087141]
34. Kim RB, Wandel C, Leake B, Cvetkovi,c M, Fromm MF, Dempsey PJ, Roden MM, Belas F, Chaudhary AK, Roden DM, Wood AJ, Wilkinson GR. Interrelationship between substrates and inhibitors of human CYP3A and P-glycoprotein. Pharm. Res. 1999; 16:408–414. [PubMed: 10213372]
35. Wandel C, Kim RB, Guengerich FP, Wood AJ. Mibefradil is a P-glycoprotein substrate and a potent inhibitor of both P-glycoprotein and CYP3A in vitro. Drug Metab. Dispos. 2000; 28:895–898. [PubMed: 10901697]
36. Miyake N, Fujita R, Ishikawa M, Takayanagi M, Takayanagi Y, Sasaki K. Reversal of multidrug resistance in human leukemia K562 by tamolarizine, a novel calcium antagonist. Jpn. J. Pharmacol. 2000; 86:265–268. [PubMed: 10887958]
37. Pauli-Magnus C, von Richter O, Burk O, Ziegler A, Mettang T, Eichelbaum M, Fromm MF. Characterization of the major metabolites of verapamil as substrates and inhibitors of P-glycoprotein. J. Pharmacol. Exp. Ther. 2000; 293:376–378. [PubMed: 10773005]
38. Polli JW, Wring SA, Humphreys JE, Huang L, Morgan JB, Webster LO, Serabjit-Singh CS. Rational use of in vitro P-glycoprotein assays in drug discovery. J. Pharmacol. Exp. Ther. 2001; 299:620–628. [PubMed: 11602674]
39. Wang E, Lew K, Barecki M, Casciano CN, Clement RP, Johnson WW. Quantitative distinctions of active site molecular recognition by P-glycoprotein and cytochrome P450 3A4. Chem. Res. Toxicol. 2001; 14:1596–1603. [PubMed: 11743742]
40. Katoh M, Nakajima M, Yamazaki H, Yokoi T. Inhibitory effects of CYP3A4 substrates and their metabolites on P-glycoprotein-mediated transport. Eur. J. Pharm. Sci. 2001; 12:505–513. [PubMed: 11231118]

41. Leonessa F, Kim JH, Ghiorghis A, Kulawiec RJ, Hammer C, Talebian A, Clarke R. C-7 analogues of progesterone as potent inhibitors of the P-glycoprotein efflux pump. J. Med. Chem. 2002; 45:390–398. [PubMed: 11784143]
42. Mahar Doan KM, Humphreys JE, Webster LO, Wring SA, Shampine LJ, Serabjit-Singh CJ, Adkison KK, Polli JW. Passive permeability and P-glycoprotein-mediated efflux differentiate central nervous system (CNS) and non-CNS marketed drugs. J. Pharmacol. Exp. Ther. 2002; 303:1029–1037. [PubMed: 12438524]
43. Che XF, Nakajima Y, Sumizawa T, Ikeda R, Ren XQ, Zheng CL, Mukai M, Furukawa T, Haraguchi M, Gao H, Sugimoto Y, Akiyama S. Reversal of P-glycoprotein mediated multidrug resistance by a newly synthesized 1,4-benzothiazipine derivative, JTV-519. Cancer Lett. 2002; 187:111–119. [PubMed: 12359358]
44. Ekins S, Kim RB, Leake BF, Dantzig AH, Schuetz EG, Lan LB, Yasuda K, Shepard RL, Winter MA, Schuetz JD, Wikel JH, Wrighton SA. Three-dimensional quantitative structure-activity relationships of inhibitors of P-glycoprotein. Mol. Pharmacol. 2002; 61:964–973. [PubMed: 11961113]
45. Ekins S, Kim RB, Leake BF, Dantzig AH, Schuetz EG, Lan LB, Yasuda K, Shepard RL, Winter MA, Schuetz JD, Wikel JH, Wrighton SA. Application of three-dimensional quantitative structure-activity relationships of P-glycoprotein inhibitors and substrates. Mol. Pharmacol. 2002; 61:974–981. [PubMed: 11961114]
46. Merino G, Alvarez AI, Prieto JG, Kim RB. The anthelminthic agent albendazole does not interact with p-glycoprotein. Drug Metab. Dispos. 2002; 30:365–369. [PubMed: 11901088]
47. Perloff MD, Störmer E, von Moltke LL, Greenblatt DJ. Rapid assessment of P-glycoprotein inhibition and induction in vitro. Pharm. Res. 2003; 20:1177–1184. [PubMed: 12948015]
48. Schwab D, Fischer H, Tabatabaei A, Poli S, Huwyler J. Comparison of in vitro P-glycoprotein screening assays: recommendations for their use in drug discovery. J. Med. Chem. 2003; 46:1716–1725. [PubMed: 12699389]
49. Tolle-Sander S, Grill A, Joshi H, Kapil R, Persiani S, Polli JE. Characterization of dexloxiglumide in vitro biopharmaceutical properties and active transport. J. Pharm. Sci. 2003; 92:1968–1980. [PubMed: 14502537]
50. Toyobuku H, Tamai I, Ueno K, Tsuji A. Limited influence of P-glycoprotein on small-intestinal absorption of cilostazol, a high absorptive permeability drug. J. Pharm. Sci. 2003; 92:2249–2259. [PubMed: 14603510]
51. Choi CH, Kim JH, Kim SH. Reversal of P-glycoprotein-mediated MDR by 5,7,3',4',5'-pentamethoxyflavone and SAR. Biochem. Biophys. Res. Commun. 2004; 320:672–679. [PubMed: 15240100]
52. Minderman H, O'Loughlin KL, Pendyala L, Baer MR. VX-710 (biricodar) increases drug retention and enhances chemosensitivity in resistant cells overexpressing P-glycoprotein, multidrug resistance protein, and breast cancer resistance protein. Clin. Cancer Res. 2004; 10:1826–1834. [PubMed: 15014037]
53. Lee Y, Yeo H, Liu SH, Jiang Z, Savizky RM, Austin DJ, Cheng YC. Increased anti-P-glycoprotein activity of baicalein by alkylation on the A ring. J. Med. Chem. 2004; 47:5555–5566. [PubMed: 15481991]
54. Griffin J, Fletcher N, Clemence R, Blanchflower S, Brayden DJ. Selamectin is a potent substrate and inhibitor of human and canine P-glycoprotein. J. Vet. Pharmacol. Ther. 2005; 28:257–265. [PubMed: 15953199]
55. Chen C, Mireles RJ, Campbell SD, Lin J, Mills JB, Xu JJ, Smolarek TA. Differential interaction of 3-hydroxy-3-methylglutaryl-coa reductase inhibitors with ABCB1, ABCC2, and OATP1B1. Drug Metab. Dispos. 2005; 33:537–546. [PubMed: 15616150]
56. Hayeshi R, Masimirembwa C, Mukanganyama S, Ungell AL. The potential inhibitory effect of antiparasitic drugs and natural products on P-glycoprotein mediated efflux. Eur. J. Pharm. Sci. 2006; 29:70–81. [PubMed: 16846720]
57. Keogh JP, Kunta JR. Development, validation and utility of an in vitro technique for assessment of potential clinical drug-drug interactions involving P-glycoprotein. Eur. J. Pharm. Sci. 2006; 27:543–554. [PubMed: 16406207]

58. Zhu HJ, Wang JS, Markowitz JS, Donovan JL, Gibson BB, Gefroh HA, Devane CL. Characterization of P-glycoprotein inhibition by major cannabinoids from marijuana. J. Pharmacol. Exp. Ther. 2006; 317:850–857. [PubMed: 16439618]
59. Huang Y, Blower PE, Liu R, Dai Z, Pham AN, Moon H, Fang J, Sadée W. Chemogenomic analysis identifies geldanamycins as substrates and inhibitors of ABCB1. Pharm. Res. 2007; 24:1702–1712. [PubMed: 17457659]
60. Kaiser D, Terfloth L, Kopp S, Schulz J, de Laet R, Chiba P, Ecker GF, Gasteiger J. Self-organizing maps for identification of new inhibitors of P-glycoprotein. J. Med. Chem. 2007; 50:1698–1702. [PubMed: 17352460]
61. Colabufo NA, Berardi F, Perrone R, Rapposelli S, Digiacomo M, Vanni M, Balsamo A. 2-[(3-Methoxyphenylethyl)phenoxy]-based ABCB1 inhibitors: effect of different basic side-chains on their biological properties. J. Med. Chem. 2008; 51:7602–7612. [PubMed: 19053888]
62. Winter SS, Lovato ML, Khawaja HM, Edwards BS, Steele ID, Young SM, Oprea TI, Skylar LA, Larson RS. High-Throughput Screening for Daunorubicin-Mediated Drug Resistance Identifies Mometasone Furoate as a Novel ABCB1-Reversal Agent. J. Biomol. Screening. 2008; 13:185–193.
63. von Richter O, Glavinas H, Krajcsi P, Liehner S, Siewert B, Zech K. A novel screening strategy to identify ABCB1 substrates and inhibitors. Naunyn-Schmiedeberg's Arch. Pharmacol. 2009; 379:11–26. [PubMed: 18758752]
64. Kwak JO, Lee SH, Lee GS, Kim MS, Ahn YG, Lee JH, Kim SW, Kim KH, Lee MG. Selective inhibition of MDR1 (ABCB1) by HM30181 increases oral bioavailability and therapeutic efficacy of paclitaxel. Eur. J. Pharmacol. 2010; 627:92–98. [PubMed: 19903471]
65. NIHM Psychoactive Drug Screening Program. [accessed April 2010]. http://pdsp.med.unc.edu/indexR.html
66. Olah, M.; Rad, R.; Ostopovici, L.; Bora, A.; Hadaruga, N.; Hadaruga, D.; Moldovan, R.; Fulias, A.; Mracec, M.; Oprea, TI. WOMBAT and WOMBAT-PK: Bioactivity Databases for Lead and Drug Discovery. In: Schreiber, SL.; Kapoor, TM.; Wess, G., editors. Chemical Biology: From Small Molecules to Systems Biology and Drug Design. Wiley-VCH; 2007. p. 760-786.
67. The chEMBL Database. [accessed April 2010]. http://www.ebi.ac.uk/chembl/
68. Klopman G, Shi LM, Ramu A. Quantitative structure-activity relationship of multidrug resistance reversal agents. Mol. Pharmacol. 1997; 52:323–324. [PubMed: 9271356]
69. O'Connell CE, Salvato KA, Meng Z, Littlefield BA, Schwartz CE. Synthesis and evaluation of hapalosin and analogs as MDR-reversing agents. Bioorg. Med. Chem. Lett. 1999; 9:1541–1546. [PubMed: 10386932]
70. Hiessböck R, Wolf C, Richter E, Hitzler M, Chiba P, Kratzel M, Ecker G. Synthesis and in vitro multidrug resistance modulating activity of a series of dihydrobenzopyrans and tetrahydroquinolines. J. Med. Chem. 1999; 42:1921–1926. [PubMed: 10354400]
71. Sarshar S, Zhang C, Moran EJ, Krane S, Rodarte JC, Benbatoul KD, Dixon R, Mjalli AM. 2,4,5-Trisubstituted imidazoles: novel nontoxic modulators of P-glycoprotein mediated multidrug resistance. Part 1. Bioorg. Med. Chem. Lett. 2000; 10:2599–2601. [PubMed: 11128632]
72. Zhang C, Sarshar S, Moran EJ, Krane S, Rodarte JC, Benbatoul KD, Dixon R, Mjalli AM. 2,4,5-Trisubstituted imidazoles: novel nontoxic modulators of P-glycoprotein mediated multidrug resistance. Part 2. Bioorg. Med. Chem. Lett. 2000; 10:2603–2605. [PubMed: 11128633]
73. Fleischer R, Wiese M. Three-dimensional quantitative structure-activity relationship analysis of propafenone-type multidrug resistance modulators: influence of variable selection on test set predictivity. J. Med. Chem. 2003; 46:4988–5004. [PubMed: 14584949]
74. Hegde R, Thimmaiah P, Yerigeri MC, Krishnegowda G, Thimmaiah KN, Houghton PJ. Anti-calmodulin acridone derivatives modulate vinblastine resistance in multidrug resistant (MDR) cancer cells. Eur. J. Med. Chem. 2004; 39:161–167. [PubMed: 14987825]
75. Wang S, Folkes A, Chuckowree I, Cockcroft X, Sohal S, Miller W, Milton J, Wren SP, Vicker N, Depledge P, Scott J, Smith L, Jones H, Mistry P, Faint R, Thompson D, Cocks S. Studies on pyrrolopyrimidines as selective inhibitors of multidrug-resistance-associated protein in multidrug resistance. J. Med. Chem. 2004; 47:1329–1338. [PubMed: 14998323]

76. Bisi A, Gobbi S, Rampa A, Belluti F, Piazzi L, Valenti P, Gyemant N, Molnár J. New potent P-glycoprotein inhibitors carrying a polycyclic scaffold. J. Med. Chem. 2006; 49:3049–3051. [PubMed: 16722621]
77. Chan KF, Zhao Y, Burkett BA, Wong IL, Chow LM, Chan TH. Flavonoid dimers as bivalent modulators for P-glycoprotein-based multidrug resistance: synthetic apigenin homodimers linked with defined-length poly(ethylene glycol) spacers increase drug retention and enhance chemosensitivity in resistant cancer cells. J. Med. Chem. 2006; 49:6742–6759. [PubMed: 17154505]
78. Richter M, Molnár J, Hilgeroth A. Biological evaluation of bishydroxymethyl-substituted cage dimeric 1,4-dihydropyridines as a novel class of p-glycoprotein modulating agents in cancer cells. J. Med. Chem. 2006; 49:2838–2840. [PubMed: 16640345]
79. Labrie P, Maddaford SP, Fortin S, Rakhit S, Kotra LP, Gaudreault RC. A comparative molecular field analysis (CoMFA) and comparative molecular similarity indices analysis (CoMSIA) of anthranilamide derivatives that are multidrug resistance modulators. J. Med. Chem. 2006; 49:7646–7660. [PubMed: 17181148]
80. Dzubák P, Hajdúch M, Gazák R, Svobodová A, Psotová J, Walterová D, Sedmera P, Kren V. New derivatives of silybin and 2,3-dehydrosilybin and their cytotoxic and P-glycoprotein modulatory activity. Bioorgan. Med. Chem. 2006; 14:3793–3810.
81. Labrie P, Maddaford SP, Lacroix J, Catalano C, Lee DK, Rakhit S, Gaudreault RC. In vitro activity of novel dual action MDR anthranilamide modulators with inhibitory activity on CYP-450 (Part 2). Bioorgan. Med. Chem. 2007; 15:3854–3856.
82. Müller H, Klinkhammer W, Globisch C, Kassack MU, Pajeva IK, Wiese M. New functional assay of P-glycoprotein activity using Hoechst 33342. Bioorgan. Med. Chem. 2007; 15:7470–7479.
83. Colabufo NA, Berardi F, Perrone R, Rapposelli S, Digiacomo M, Vanni M, Balsamo A. Synthesis and biological evaluation of (hetero)arylmethyloxy- and arylmethylamine-phenyl derivatives as potent P-glycoprotein modulating agents. J. Med. Chem. 2008; 51:1415–1422. [PubMed: 18257545]
84. Müller H, Pajeva IK, Globisch C, Wiese M. Functional assay and structure-activity relationships of new third-generation P-glycoprotein inhibitors. Bioorgan. Med. Chem. 2008; 16:2448–2462.
85. PubMed. [Accessed April 2010]. http://www.ncbi.nlm.nih.gov/pubmed
86. Ecker G, Huber M, Schmid D, Chiba P. The importance of a nitrogen atom in modulators of multidrug resistance. Mol. Pharmacol. 1999; 56:791–796. [PubMed: 10496963]
87. Carosati E, Sciabola S, Cruciani G. Hydrogen Bonding Interactions of Covalently Bonded Fluorine Atoms: From Crystallographic Data to a New Angular Function in the GRID Force Field. J. Med. Chem. 2004; 47:5114–5125. [PubMed: 15456255]
88. Cross S, Cruciani G. Molecular fields in drug discovery: Getting old or reaching maturity. Drug Discov.Today. 2010; 15:23–32. [PubMed: 19150413]
89. Milletti F, Storchi L, Sforna G, Cruciani G. New and original pK_a prediction method using grid molecular interaction fields. J. Chem. Inf. Model. 2007; 47:2172–2181. [PubMed: 17910431]
90. Milletti F, Storchi L, Sforna G, Cross S, Cruciani G. Tautomer enumeration and stability prediction for virtual screening on large chemical databases. J. Chem. Inf. Model. 2009; 49:68–75. [PubMed: 19123923]
91. Von Itzstein M, Wu W, Kok GB, Pegg MS, Dyason JC, Jin B, Phan TV, Smythe ML, White HF, Oliver SW, Colman PM, Varghese JN, Ryan DM, Woods JM, Bethell RC, Hotham VJ, Cameron JM, Penn CR. Rational design of potent sialidase-based inhibitors of influenza virus replication. Nature. 1993; 363:418–423. [PubMed: 8502295]
92. Ahlström MM, Ridderström M, Luthman K, Zamora I. Virtual screening and scaffold hopping based on GRID molecular interaction fields. J. Chem. Inf. Model. 2005; 45:1313–1323. [PubMed: 16180908]
93. Bergmann R, Linusson A, Zamora I. SHOP: Scaffold hopping by GRID-based similarity searches. J. Med. Chem. 2007; 50:2708–2717. [PubMed: 17489578]
94. Carosati E, Budriesi R, Ioan P, Ugenti MP, Frosini M, Fusi F, Corda G, Cosimelli B, Spinelli D, Chiarini A, Cruciani G. Discovery of novel and cardioselective diltiazem-like calcium channel blockers via virtual screening. J. Med. Chem. 2008; 51:5552–5565. [PubMed: 18754582]

95. Pastor M, Cruciani G, McLay I, Pickett S, Clementi S. Gridindependent descriptors (GRIND): A novel class of alignmentindependent three-dimensional molecular descriptors. J. Med. Chem. 2000; 43:3233–3243. [PubMed: 10966742]

96. Fontaine F, Pastor M, Zamora I, Sanz F. Anchor-GRIND: Filling the gap between standard 3D QSAR and the GRid-Independent descriptors. J. Med. Chem. 2005; 48:2687–2694. [PubMed: 15801859]

97. Sciabola S, Carosati E, Cucurull-Sanchez L, Baroni M, Mannhold R. Novel TOPP descriptors in 3D-QSAR analysis of apoptosis inducing 4-aryl-4H-chromenes: comparison versus other 2D- and 3D-descriptors. Bioorgan. Med. Chem. 2007; 15:6450–6462.

98. Sciabola S, Carosati E, Baroni M, Mannhold R. Comparison of Ligand-Based and Structure-Based 3D QSAR Approaches: A Case Study on (aryl)bridged 2-aminobenzonitriles. J. Med. Chem. 2005; 48:3756–3767. [PubMed: 15916427]

99. Tedeschi G, Nonnisa S, Strumboa B, Cruciani G, Carosati E, Negri A. On the catalytic role of the active site residue E121 of E. coli L-aspartate oxidase. Biochimie. 2010; 92:1335–1342. [PubMed: 20600565]

100. Cruciani G, Pastor M, Guba W. VolSurf: A new tool for the pharmacokinetic optimization of lead compounds. Eur. J. Pharm. Sci. 2000; 11:S29–S39. [PubMed: 11033425]

101. Cruciani G, Carosati E, De Boeck B, Ethirajulu K, Mackie C, Howe T, Vianello R. MetaSite: Understanding metabolism in human cytochromes from the perspective of the Chemist. J. Med. Chem. 2005; 48:6970–6979. [PubMed: 16250655]

102. Ahlström MM, Ridderström M, Zamora I, Luthman K. CYP2C9 structure-metabolism relationships: Optimizing the metabolic stability of COX-2 inhibitors. J. Med. Chem. 2007; 50:4444–4452. [PubMed: 17696334]

103. Carosati E, Cruciani G, Chiarini A, Budriesi R, Ioan P, Spisani R, Spinelli D, Cosimelli B, Fusi F, Frosini M, Matucci R, Gasparrini F, Ciogli A, Stephens PJ, Devlin FJ. Calcium channel antagonists discovered by a multidisciplinary approach. J. Med. Chem. 2006; 49:5206–5216. [PubMed: 16913709]

104. Carosati E, Mannhold R, Wahl P, Hansen JB, Fremming T, Zamora I, Cianchetta G, Baroni M. Virtual screening for novel openers of pancreatic KATP channels. J. Med. Chem. 2007; 50:2117–2126. [PubMed: 17425298]

105. Cross S, Baroni M, Carosati E, Benedetti P, Clementi S. FLAP: GRID Molecular Interaction Fields in Virtual Screening. Validation using the DUD Data Set. J. Chem. Inf. Model. 2010; 50:1442–1450. [PubMed: 20690627]

106. Carosati E, Sforna G, Pippi M, Marverti G, Ligabue A, Guerrieri D, Piras S, Guaitoli G, Luciani R, Costi MP, Cruciani G. Ligand-Based Virtual Screening and ADME-Tox Guided Approach to Identify Triazolo-quinoxalines as Folate Cycle Inhibitors. Bioorgan. Med. Chem. 2010; 18:7773–7785.

107. Brincat JP, Carosati E, Sabatini S, Manfroni G, Fravolini A, Raygada JL, Patel D, Kaatz GW, Cruciani G. Discovery of Novel Inhibitors of the NorA Multidrug Transporter of Staphylococcus aureus. J. Med. Chem. DOI: 10.1021/jm1011963.

108. Consell G, Baubichon-Corty H, Dayan G, Barron D, Di Pietro A. Flavonois: a class of modulators with bifunctional interactions at vivinal ATP- and steroid-binding sites on mouse P-glycoprotein. Proc. Natl. Acad. USA. 1998; 95:9831–9836.

109. The Open Babel Package, version 2.3.0. [accessed November 2010]. http://openbabel.sourceforge.net/

110. [accessed November 2010]. http://www.ailab.si/orange/

111. Leach AR, Gillet VJ, Lewis RA, Taylor R. Three Dimensional Pharmacophore Methods in Drug Discovery. J. Med. Chem. 2010; 53:539–558. [PubMed: 19831387]

112. Wermuth CG, Ganellin CR, Lindeberg P, Mitscher LA. Glossary of terms used in medicinal chemistry (IUPAC Recomendations 1998). Pure Appl. Chem. 1998; 70:1129–1143.

113. Manthey JA. Biological properties of flavonoids pertaining to inflammation. Microcirculation. 2000; 7:S29–S34. [PubMed: 11151968]

114. Boccard J, Bajot F, Di Pietro A, Rudaz S, Boumendjel A, Nicolle E, Carrupt P. A 3D linear solvation energy model to quantify the affinity of flavonoid derivatives toward P-glycoprotein. Eur. J. Pharm. Sci. 2009; 36:254–264. [PubMed: 18955135]

115. http://www.sigmaaldrich.com

116. Weaver JL, Szabo G Jr, Pine PS, Gottesman MM, Goldenberg S, Aszalos A. The effect of ion channel blockers, immunosuppressive agents, and other drugs on the activity of the multi-drug transporter. Int. J. Cancer. 1993; 54:456–461. [PubMed: 7685326]

117. Saponara S, Kawase M, Shah A, Motohashi N, Molnar J, Ugocsai K, Sgaragli G, Fusi F. 3,5-Dibenzoyl-4-(3-phenoxyphenyl)-1,4-dihydro-2,6-dimethylpyridine (DP7) as a new multidrug resistance reverting agent devoid of effects on vascular smooth muscle contractility. Br. J. Pharmacol. 2004; 141:415–422. [PubMed: 14718255]

118. Wang EJ, Casciano CN, Clement RP, Johnson WW. In vitro flow cytometry method to quantitatively assess inhibitors of P-glycoprotein. Drug Metab. Dispos. 2000; 28:522–528. [PubMed: 10772630]

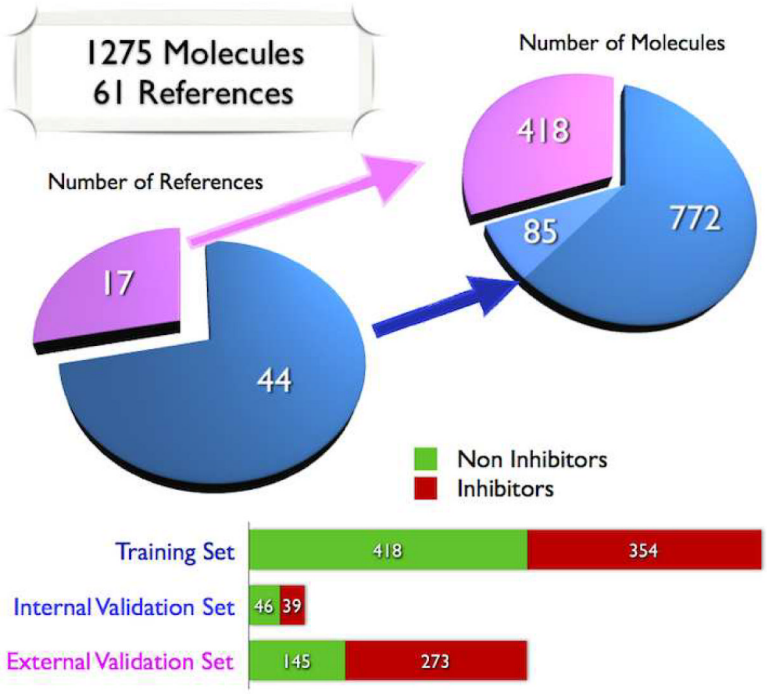

Figure 1.

Data set selection. References and the corresponding molecules are differently coloured if they belong to the Training set and Internal Validation sets (blue) or External Validation set (magenta). In addition, for each set the division between Pgp inhibitors (red) and non-inhibitors (green) is shown with the horizontal bars. All data are available as Supporting Information.

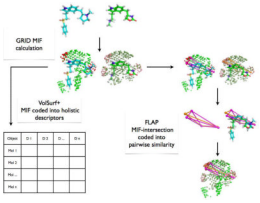

Figure 2.

Flow chart of the GRID-based technologies used. While VolSurf+ elaborates MIFs to compute holistic molecular descriptors suitable for modeling pharmacokinetic properties, FLAP extracts hotspots from the GRID MIFs, combining them in quadruplets. Each quadruplet of the molecule A is overlaid with each quadruplet of the molecule B and for each match a score associated to the 3D-superposition of the two molecules is calculated which estimates how much the MIFs are intersected. At the end of the process, only the best score obtained, which corresponds to the best superimposition, is used to assess the 3D-similarity between the two molecules.

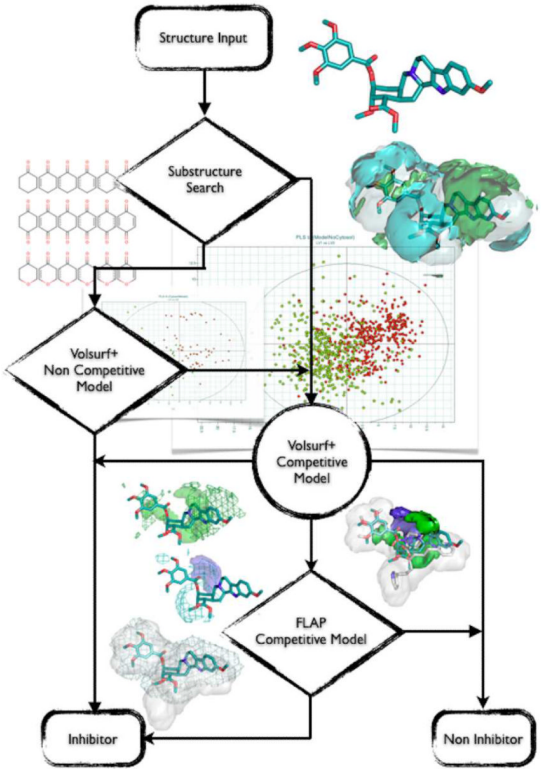

Figure 3.
Flow chart of the Composite Model.

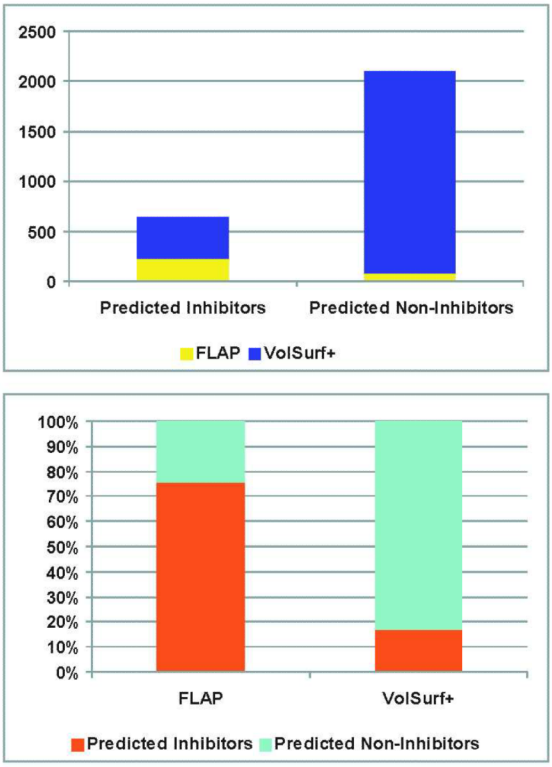

Figure 4.
Schema of the prediction of the DRUGS data set of drugs (about 2,700 molecules).

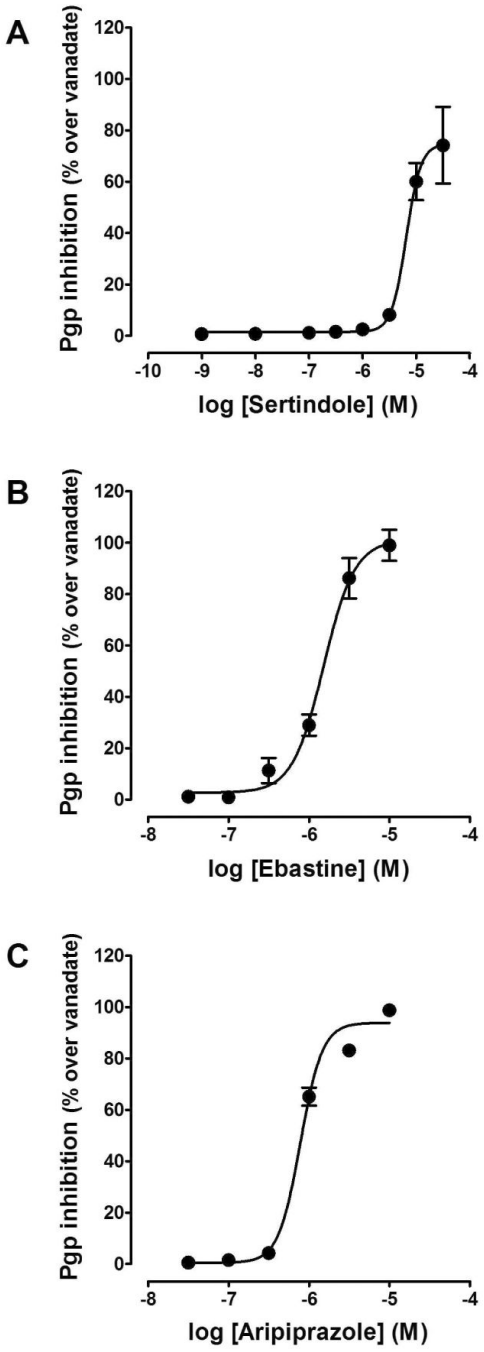

Figure 5.

Concentration-response curve of the inhibition of Pgp-mediated R123 efflux from L5178 MDR1 cells by Sertindole (panel A), Ebastine (panel B) and Aripiprazole (panel C) IC_{50} for the Pgp inhibitors was reported in Table 3. Data are depicted as mean ±e.s.m. of at least three independent experiments run in triplicate.

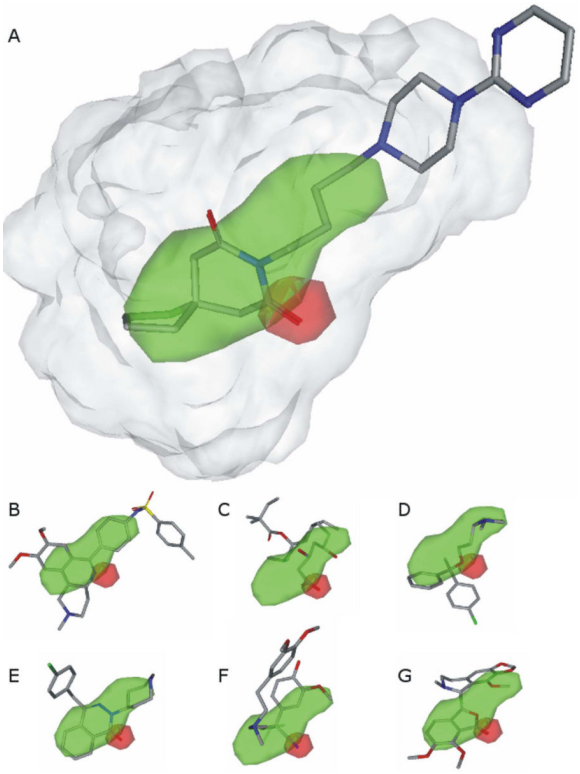

Figure 6.
FLAP pharmacophore hypothesis found using the FLAP-Pharm Procedure. Hydrophobic regions (where a favourable hydrophobic interaction might occur) are represented by the green contour, while HB acceptor regions are shown as red contours. The shape is coloured in pale grey. Buspirone (A) is superposed to the pharmacophore for reference. The buspirone ring on the right is probably exposed toward solvent. Other inhibitors (B=Tolafentrine; C=Simvastatin; D=Clemastine; E=Desmethylazelastine; F=D703; G=Noscapine) are reported to show the degree of complementarity with the proposed pharmacophore.

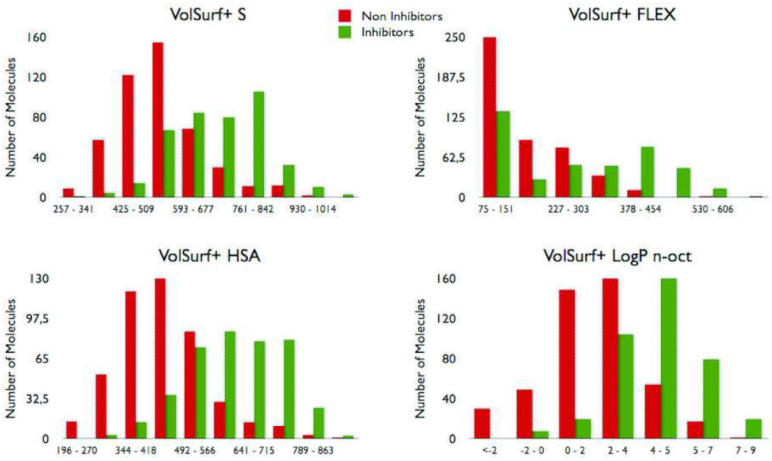

Figure 7.

Distribution of some VolSurf+ descriptors for Pgp non-inhibitors (grey) and inhibitors (black). Descriptors reported are molecular surface (S), flexibility (FLEX), hydrophobic surface area (HSA) and coefficient of partitioning in octanol/water (LogPn-oct).

Table 1

Criteria used to classify molecules either as Pgp non-inhibitor or inhibitor.

	IC_{50} (μM)	% Inhibition[a]	% Inhibition[b]
Non-inhibitor	≥ 100	< 10	< 12
Inhibitor	≤ 15	> 25	> 30

[a] % Inhibition respect to not transfected cell line or maximum inhibition.[38]

[b] For the particular case of PDSP different thresholds were defined.[65]

Table 2

Model performance in the different data sets.

	Accuracy[a]	Sensitivity[a]	Specificity[a]	Unweighted Cohen's kappa[a]
Training	0.88	0.84	0.91	0.75
Internal Validation	0.85	0.82	0.87	0.69
External Validation	0.86	0.90	0.80	0.70

[a]Percent values refer to the number of correct predictions with respect to the total number of molecules (N=772). Since Pgp inhibition is the target of the model, sensitivity refers to the prediction of inhibitors and specificity of non-inhibitors. All the statistict were derived using the True Positives, True Negatives, False Positive and False Negatives as reported in the Supporting Information.

Table 3

Inhibition of Pgp-mediated cell efflux of R123 in mouse T lymphoma L5178 MDR1 cells by the nine molecules of the blind set, Cyclosporine A used as control.

Molecule[a]	Prediction (Classification)	Exp data		
		αmax[b]	IC_{50} (M)[c]	Classification[d]
Cyclosporine A[e]	N.A.[e]	0.92[f]	6.5×10^{-7}	Pgp Inhibitor
Aripiprazole	Pgp Inhibitor	0.99[f]	7.8×10^{-7}	Pgp Inhibitor
Ebastine	Pgp Inhibitor	0.99[f]	1.5×10^{-6}	Pgp Inhibitor
Sertindole	Pgp Inhibitor	0.74[f,g]	6.5×10^{-6}[f]	Pgp Inhibitor
Repaglinide	Pgp Inhibitor	0.35	N.D.[h]	Pgp Inhibitor
Ziprasidone	Pgp Inhibitor	0.19	N.D.[h]	Pgp weak inhibitor
Aprindine	Pgp Inhibitor	0.16	N.D.[h]	Pgp weak inhibitor
Alprenolol	Pgp Non-Inhibitor	0.05[i]	N.D.[h]	Pgp Non-Inhibitor
Nateglinide	Pgp Non-Inhibitor	0	N.D.[h]	Pgp Non-Inhibitor
Ticarcillin	Pgp Non-Inhibitor	0	N.D.[h]	Pgp Non-Inhibitor

[a] Molecular structures are given as Supporting Information.

[b] α_{max}, expresses the efficacy of the inhibitor and it varies between 0 (in the absence of the inhibitor) and 1 (when the amount of R123 found in L5178 MDR1 cells was comparable to that determined in the presence of 5×10^{-3} M sodium orthovanadate). The values reported represent the efficacy determined at 1×10^{-4} M inhibitor concentration.

[c] IC_{50} measures inhibitor potency and represents the concentration that causes a half-maximal increase (α=0.5) in intracellular concentration of R123.

[d] The classification was coherent with the thresholds used in the dataset collection.

[e] Cyclosporine was used as control. Preliminary data were presented at XIV National Congress of PhD Student in Pharmacological Sciences, Siena (Italy), 20–23 September 2010. It was in the Training set, so no prediction is provided.

[f] See also Figure 5.

[g] apparent IC_{50}.

[h] N.D. = Not Detectable.